

The Stereochemical Effect of 6s² Lone-Pair Electrons: The Crystal Structure of a New Lead Bismuth Oxyphosphate Pb₄BiO₄PO₄

Sophie Giraud,* † Jean-Pierre Wignacourt,* Michel Drache,* Guy Nowogrocki,* and Hugo Steinfink†¹

*Laboratoire de Cristallographie et Physicochimie du Solide, URA CNRS 452, ENSCL, BP 108, 59652 Villeneuve d'Ascq Cedex, France; and

†Texas Materials Institute, Department of Chemical Engineering, University of Texas, Austin, Texas 78712

Received April 2, 1998, in revised form July 15, 1998; accepted July 23, 1998

Pb₄BiO₄PO₄ was prepared by heating a stoichiometric mixture of (NH₄)₂HPO₄, PbO, and Bi₂O₃ at 700°C for 4 days with intermediate grinding. The material melts congruently at 805°C; single crystals were obtained by slow cooling of a melt. The compound is triclinic, P $\bar{1}$, $a = 6.215(1)$ Å, $b = 7.440(2)$ Å, $c = 10.498(2)$ Å, $\alpha = 100.19(1)^\circ$, $\beta = 103.73(1)^\circ$, $\gamma = 90.05(1)^\circ$, $Z = 2$. The structure refinement converged to $R = 0.0485$. Bi is bonded to 4 O at distances varying from 2.16(3) Å to 2.53(3) Å and two bonds at 3.10(3) Å and 3.15(3) Å. Five atoms form an almost perfect pentagon parallel to (001) with an apical Bi–O bond nearly perpendicular to the pentagonal plane. Presumably the lone pair points to the empty apex to complete a pentagonal bipyramid. Pb(1) is bonded to seven oxygen atoms. Five of these bonds are less than 2.9 Å, while two are 3.12(3) Å and 3.16(3) Å. Four oxygen atoms constitute the equatorial plane of an octahedron with Pb(1) slightly out of that plane. The apex oxygen atoms are tilted in the same direction away from the normal to the equatorial plane. One triangular face is capped by an oxygen atom while another triangular face is open and the lone pair electrons cap this face. Pb(2), Pb(3), and Pb(4) have similar coordination polyhedra. The average of the four P–O bonds is 1.53(5) Å. The Pb–O framework is related to that of tetragonal PbO and the structure is related to that of Pb₅SO₈. The valence bond sums for two of the Pb atoms are 2.63 and 2.32, while the other two Pb atoms have the more expected values, 2.14 and 2.06. The valence bond sum for Bi is 2.14, much less than the expected trivalent oxidation state. Van der Waals contacts exist between the two Pb with the increased oxidation states and Bi but no contacts exist between the other two Pb and Bi. Where van der Waals contacts are present the Pb 6s² energy levels overlap the empty Bi 6p energy levels so that electron transfer into the Bi 6p levels from Pb occurs. The electrons are not itinerant because of the large atomic separations and the material remains insulating. © 1999 Academic Press

INTRODUCTION

The discovery that Bi₄V₂O₁₁ is a good oxide ion conductor has led to intense research on this compound. Numerous attempts have been reported to improve the ion conductivity by isovalent and aliovalent substitution of the transition metal and of bismuth. The Bi–P(V)–O system (1–4) and the pseudoternary systems Bi₂O₃–PbO–M₂O₅, where $M = P, V, As$, have been extensively investigated (5–7) in the expectation that some of the compounds will display interesting physical properties such as improved anionic conduction. Mizrahi *et al.* (5) described new phases with $M = V$ and, in particular, Pb₄BiVO₈. Unfortunately the crystals were of poor quality and no structure for this compound was determined. Surprisingly, numerous compounds with related stoichiometries, Pb₅SO₈ (8, 9), Pb₅CrO₈ (10, 11), Pb₅SeO₈ (11), Pb₅(Cr_{1-x}S_x)O₈ (12), and Pb₅MoO₈ (13), were only partially characterized due to commensurate and incommensurate modulations present in their structures. Precise oxygen atomic positions were not even available for Pb₅SO₈, which was widely studied because of applications in lead-acid battery technology. Only recently has its crystal structure been solved (14) and shown to be closely related to the structure of PbO. We report here the structure of a new compound, Pb₄BiO₄PO₄ (hereafter Pb₄BiPO₈), with a similar stoichiometry.

EXPERIMENTAL

Polycrystalline samples were prepared by solid state reaction of stoichiometric proportions of (NH₄)₂HPO₄, PbO, and Bi₂O₃. Prior to use the oxides were preheated overnight at 600°C to remove any carbonate. After thorough grinding, the powder was slowly heated at 300°C until the diammonium hydrogen phosphate had completely decomposed. The reaction was completed after annealing at 700°C for 4 days with intermediate grinding. The samples were examined by X-ray diffraction with a Guinier-de Wolff

¹To whom correspondence should be addressed.

camera and $\text{CuK}\alpha$ radiation. A final pattern was recorded on an automated D5000 Siemens diffractometer and completely indexed using TREOR (15). Density measurements were performed with an automated Micromeritics Accucyc 1330 gas pycnometer equipped with a 1 cm^3 cell. Differential thermal analysis (DTA) was done on a Du Pont 1090B thermal analyzer using a 1600 differential thermal analysis cell with a heating rate of 5°C min^{-1} . The possibility of phase transitions was checked with a high temperature X-ray diffraction (HTXRD) Guinier-Lenné camera at a heating rate of $20^\circ\text{C min}^{-1}$.

Single crystals of Pb_4BiPO_8 were obtained by melting of polycrystalline samples and slow cooling in a gold crucible. Pb_4BiPO_8 melts congruently at 805°C without an intermediate phase transition. The temperature was raised to 840°C at 250°C/h , held at 840°C for 3 h, cooled to 725°C at 1°C/h and then furnace cooled to room temperature. The crystals are light yellow needles. Weissenberg photographs were used to determine the quality of the crystals. The data for the structure determination were recorded on a Siemens P4 diffractometer. The pertinent data are summarized in Table 1. An absorption correction using SHELXTL-PLUS (16) was applied. SHELXS-86 (17) was used to find the structure solution and the refinement was performed with SHELXL93 (18). The structure was solved using the Patterson method and refined by full-matrix least squares. The Pb, Bi, and P atoms were refined anisotropically, while O atoms were refined isotropically. The least-squares refinement was based on 1494 observed reflections, $I > 2\sigma(I)$, and 88 variable parameters and converged to $R = 0.0485$.

RESULTS

All observed lines of the powder pattern were indexed using TREOR. Lattice constants indicated the isostructural nature of Pb_4BiPO_8 and Pb_4BiVO_8 (5). The parameters were refined by least squares to $a = 6.229(2)\text{ \AA}$, $b = 7.433(3)\text{ \AA}$, $c = 10.494(2)\text{ \AA}$, $\alpha = 100.12(2)^\circ$, $\beta = 103.88(2)^\circ$, $\gamma = 90.14(2)^\circ$ and differ slightly from those obtained from the single crystal (Table 1). The figures of merit were $F(30) = 29.3(0.015, 0.68)$ and $M(20) = 20.9(3.1015, 32)$ (15). Table 2 lists the indexed powder X-ray diffraction pattern. The measured density, $\rho = 8.636\text{ g/cm}^3$, yields two formula weights per unit cell. DTA and HTXRD investigations did not show any phase transition occurring between room temperature and the melting temperature at 805°C .

Initially neither a Patterson map nor direct methods yielded a valid structural model. A trial model was constructed in the acentric space group P1. Two Pb atoms were first introduced in $0\ 0\ 0$ and $0\ 1/2\ 0$ positions and the remaining 6 Pb and 2 Bi atoms were successively introduced and refined in positions identified from the Patterson map. At this stage the refinement converged to $R = 0.14$. A

TABLE 1
Crystal Data and Intensity Collection

Crystallographic data	
Formula	Pb_4BiPO_8
Color	Light yellow
Crystal system	Triclinic
Space group	$\text{P}\bar{1}$
a (Å)	6.215(1)
b (Å)	7.440(2)
c (Å)	10.498(2)
α	$100.19(1)^\circ$
β	$103.73(1)^\circ$
γ	$90.05(1)^\circ$
Volume (Å ³)	463.6
Z	2
Formula weight (g/mol)	1196.71
Measured density (g/cm ³)	8.64
Calculated density (g/cm ³)	8.58
Intensity collection	
Diffractometer	Siemens P4
Radiation (Å)	$\text{MoK}\alpha$, $\lambda = 0.7107$
Monochromator	Graphite
Temperature (°C)	23
Scan method	ω , 1°
θ Range	$2.03\text{--}27.48^\circ$
Data collected	$-8 \leq h \leq 7$, $-9 \leq k \leq 9$, $0 \leq l \leq 13$
No of reflections measured/independent	2712/2126
No of unique reflections $I > 2\sigma(I)$	1494
μ (cm ⁻¹)	915
R_{int}	0.0438
Absorption correction	SHELXTL-PLUS
Transmission factor	0.02612 – 0.08674
Indices of single crystal faces h, k, l /dimensions (mm)	$\bar{1}00/0.02$; $100/0.02$; $010/0.12$; $0\bar{1}0/0.12$; $001/0.02$; $00\bar{1}/0.02$;
Refinement	
Parameters varied	88
Refinement method	Least squares on F^2
$R(F)$	0.0485(obs)/0.0823(all)
$R_w(F^2)$	0.1011(obs)/0.1159(all)
$w = 1/(\sigma^2(\text{Fo}^2) + (0.0493P)^2 + 9.2976P)$ with $P = (\text{Fo}^2 + 2\text{Fc}^2)/3$	
Extinction correction	0.0018×10^{-3}
GOF	1.098(obs)/1.028(all)
Max., min., $\Delta\rho$, e Å ⁻³	2.88, – 3.09

centrosymmetric origin was then identified and the appropriate translation applied to the atomic parameters. A refinement in space group $\text{P}\bar{1}$, with isotropic displacement parameters yielded a conventional $R = 0.08$. The oxygen atomic positions were now obtained from successive Fourier electron density difference maps and introduced into the refinement process. The final least squares refinement with anisotropic displacement parameters for the heavy atoms and isotropic for oxygen yielded $R = 0.0485$. Table 3 lists the final atomic parameters, Table 4 the anisotropic displacement parameters, and significant interatomic bond lengths and angles are shown in Table 5.

TABLE 2
The Powder X-Ray Diffraction Diagram of $\text{Pb}_4\text{BiO}_4\text{PO}_4$

<i>h</i>	<i>k</i>	<i>l</i>	<i>d</i> obs. Å	<i>d</i> calc. Å	I/I ₀ (%)
0	0	1	10.010	10.018	2
0	1	-1	6.494	6.493	< 1
1	0	0	6.047	6.040	< 1
1	0	-1	5.844	5.842	1
0	1	1	5.460	5.452	1
0	0	2	5.006	5.009	1
1	-1	0	4.771	4.767	< 1
1	0	1	4.694	4.691	1
0	1	-2	4.537	4.534	1
1	0	-2	4.425	4.423	< 1
1	-1	1	4.179	4.185	< 1
1	1	-2	4.015	4.015	1
0	1	2	3.821	3.821	1
1	1	1	3.748	3.747	< 1
0	2	-1	3.650	3.654	1
1	0	2	3.460	3.463	2
0	0	3	3.339	3.339	100
1	0	-3	3.280	3.281	11
0	2	-2	3.248	3.246	5
2	0	-1	3.112	3.109	1
1	2	0	3.060	3.064	1
2	0	0	3.021	3.020	13
1	-2	-1	3.016	3.017	26
2	-1	-1	2.854	2.852	1
2	-1	0	2.842	2.838	< 1
1	-2	2	2.731	2.730	19
1	0	3	2.661	2.660	9
2	0	-3	2.573	2.574	4
0	0	4	2.504	2.505	8
2	-2	0	2.384	2.383	1
2	2	-2	2.354	2.353	1
1	-3	0	2.297	2.297	3
2	-2	1	2.280	2.281	2
0	2	-4	2.268	2.267	3
1	3	0	2.225	2.224	1
2	1	2	2.156	2.158	< 1
1	0	4	2.138	2.136	1
2	-2	2	2.093	2.093	2
3	0	-1	2.074	2.074	1
1	0	-5	2.057	2.058	1
2	-1	3	2.010	2.011	2
1	-2	-4	1.943	1.943	2
2	3	-1	1.926	1.926	1
0	2	4	1.910	1.911	8
0	4	-1	1.860	1.858	4
3	2	-2	1.810	1.808	4
2	2	-5	1.792	1.791	3
1	4	-1	1.775	1.775	1
1	-3	4	1.763	1.763	< 1
3	2	0	1.730	1.730	2
1	-2	5	1.720	1.720	7
1	2	-6	1.672	1.673	2
1	1	5	1.662	1.661	1
3	2	1	1.626	1.626	4
2	-4	1	1.584	1.584	2
2	4	-3	1.565	1.566	1
4	-1	-1	1.522	1.522	3
1	0	6	1.517	1.517	1
4	0	0	1.510	1.510	2
3	-3	-3	1.478	1.478	1

Note. The lattice parameters are $a = 6.229(2)$ Å, $b = 7.443(3)$ Å, $c = 10.494(2)$ Å, $\alpha = 100.12(2)^\circ$, $\beta = 103.88(2)^\circ$, $\gamma = 90.14(2)^\circ$, $\text{CuK}\alpha$.

TABLE 3
Atomic Coordinates and Equivalent Displacement Parameters, Å², for $\text{Pb}_4\text{BiO}_4\text{PO}_4$

Atom	<i>x</i>	<i>y</i>	<i>z</i>	U_{eq}
Pb(1)	0.2386(2)	0.0351(2)	0.70334(9)	0.0181(2)
Pb(2)	0.2321(2)	0.5641(2)	0.70344(9)	0.0187(2)
Pb(3)	0.7330(2)	-0.3815(2)	0.96585(9)	0.0163(2)
Pb(4)	0.7347(2)	0.1154(2)	0.9644(1)	0.0199(3)
Bi	0.3070(2)	0.2268(2)	0.4099(1)	0.0164(2)
P	0.768(2)	0.2945(9)	0.6821(7)	0.018(2)
O(1)	0.650(3)	-0.604(2)	0.078(2)	0.011(3)
O(2)	0.645(3)	-0.106(3)	0.085(2)	0.016(3)
O(3)	0.034(3)	-0.185(3)	0.743(2)	0.017(4)
O(4)	0.001(4)	0.306(3)	0.777(2)	0.029(4)
O(5)	0.484(4)	0.188(3)	0.254(3)	0.035(5)
O(6)	0.263(4)	0.563(4)	0.400(3)	0.046(6)
O(7)	0.735(4)	0.111(4)	0.590(3)	0.041(5)
O(8)	0.588(4)	0.308(3)	0.768(2)	0.035(5)

DISCUSSION

The presence of the lone-pair electrons on Bi^{3+} and Pb^{2+} distorts the oxygen coordination polyhedra by leaving a vacancy at a corner or lengthens a bond to an anion to a van der Waals contact, usually resulting in a lowering of the crystal system and/or space group. Both of these effects are seen in this structure.

Bi is bonded to 4 O at distances varying from 2.16(3) Å to 2.53(3) Å and two bonds at 3.10(3) Å and 3.15(3) Å (Table 5). The five atoms, O(6), O(6), O(3), O(7), O(7), form an almost perfect pentagon parallel to (001) with Bi–O(5) nearly perpendicular to the pentagonal plane (Fig. 1a). Presumably the lone-pair points to the empty apex to complete a pentagonal bipyramid. If the two long Bi–O bonds are omitted from the coordination polyhedron then O(5)–O(3)–O(7)–O(6) form a trigonal bipyramid with the lone-pair occupying one apex.

Pb(1) is bonded to seven oxygen atoms. Five of these bonds are less than 2.9 Å, while two are 3.12(3) Å and 3.16(3) Å. Four oxygen atoms, O(3), O(4), O(8), O(5),

TABLE 4
Anisotropic Displacement Parameters

Atom	U_{11}	U_{22}	U_{33}	U_{23}	U_{13}	U_{12}
Pb(1)	0.0204(5)	0.0176(5)	0.0162(4)	0.0015(4)	0.0056(4)	-0.0015(4)
Pb(2)	0.0203(5)	0.0199(5)	0.0164(5)	0.0045(4)	0.0047(4)	0.0046(4)
Pb(3)	0.0142(5)	0.0133(5)	0.0229(5)	0.0027(4)	0.0082(4)	0.0007(4)
Pb(4)	0.0147(5)	0.0176(5)	0.0324(6)	0.0107(4)	0.0109(4)	0.0046(4)
Bi	0.0163(5)	0.0168(5)	0.0163(4)	0.0037(3)	0.0037(3)	0.0018(4)
P	0.019(3)	0.013(3)	0.022(3)	0.004(3)	0.006(3)	-0.001(3)

TABLE 5
Bond lengths (Å), Angles (°), and Bond Valences for Pb₄BiPO₈^a

	Bond lengths	Bond valences		Angles		Bond lengths	Bond valences
Bi–O(3)	2.32(2)	0.54	O(3)–Bi–O(5)	92(1)	Pb(1)–O(2)	2.14(2)	0.93
Bi–O(5)	2.16(3)	0.84	O(3)–Bi–O(6)	85(1)	Pb(1)–O(3)	2.23(2)	0.73
Bi–O(6)	2.53(3)	0.31	O(3)–Bi–O(6)	158(1)	Pb(1)–O(4)	2.62(2)	0.25
Bi–O(6)	3.15(3)	0.06	O(3)–Bi–O(7)	156(1)	Pb(1)–O(5)	2.41(3)	0.45
Bi–O(7)	2.52(3)	0.32	O(3)–Bi–O(7)	85(1)	Pb(1)–O(7)	3.16(3)	0.06
Bi–O(7)	3.10(3)	0.07	O(5)–Bi–O(6)	92(1)	Pb(1)–O(7)	3.12(3)	0.07
		2.14	O(5)–Bi–O(6)	88(1)	Pb(1)–O(8)	2.85(3)	0.14
			O(5)–Bi–O(7)	86(1)			2.63
			O(5)–Bi–O(7)	94(1)			
			O(6)–Bi–O(6)	73(1)	Pb(2)–O(1)	2.20(2)	0.79
			O(6)–Bi–O(7)	119(1)	Pb(2)–O(3)	2.27(2)	0.65
			O(6)–Bi–O(7)	168(1)	Pb(2)–O(4)	2.72(3)	0.19
			O(6)–Bi–O(7)	45(1)	Pb(2)–O(5)	2.46(3)	0.39
			O(6)–Bi–O(7)	117(1)	Pb(2)–O(6)	3.24(3)	0.05
			O(7)–Bi–O(7)	72(1)	Pb(2)–O(6)	3.10(3)	0.07
					Pb(2)–O(8)	2.96(3)	0.10
							2.26
P–O(4)	1.54(2)	1.23	O(4)–P–O(6)	113(2)			
P–O(6)	1.47(3)	1.49	O(4)–P–O(7)	109(2)	Pb(3)–O(1)	2.32(2)	0.57
P–O(7)	1.51(3)	1.34	O(4)–P–O(8)	109(2)	Pb(3)–O(1)	2.31(2)	0.59
P–O(8)	1.59(3)	1.08	O(6)–P–O(7)	108(2)	Pb(3)–O(2)	2.34(2)	0.54
		5.14	O(6)–P–O(8)	110(2)	Pb(3)–O(4)	3.47(2)	0.03
			O(7)–P–O(8)	108(2)	Pb(3)–O(4)	2.77(2)	0.17
					Pb(3)–O(5)	2.99(3)	0.09
Bi–Pb(1)	3.73(1)		Pb(2)–O(1)–Pb(3)	119.6(5)	Pb(3)–O(8)	2.81(2)	0.15
Bi–Pb(1)	3.74(1)		Pb(2)–O(1)–Pb(3)	105.9(5)			2.14
Bi–Pb(1)	3.74(1)		Pb(2)–O(1)–Pb(4)	114.5(5)			
Bi–Pb(2)	3.74(1)		Pb(3)–O(1)–Pb(3)	104.7(5)	Pb(4)–O(1)	2.34(2)	0.54
Bi–Pb(2)	3.72(1)		Pb(3)–O(1)–Pb(4)	106.7(4)	Pb(4)–O(2)	2.39(2)	0.47
Bi–Pb(2)	3.78(1)		Pb(3)–O(1)–Pb(4)	103.8(4)	Pb(4)–O(2)	2.29(2)	0.62
					Pb(4)–O(3)	3.02(2)	0.09
Bi–P	3.50(1)		Pb(1)–O(2)–Pb(3)	121.5(6)	Pb(4)–O(4)	3.34(3)	0.04
Bi–P	3.82(1)		Pb(1)–O(2)–Pb(4)	114.9(5)	Pb(4)–O(5)	2.98(2)	0.10
Bi–P	3.85(1)		Pb(1)–O(2)–Pb(4)	107.8(5)	Pb(4)–O(8)	2.70(3)	0.20
			Pb(3)–O(2)–Pb(4)	102.9(5)			2.06
P–Pb(1)	3.89(1)		Pb(3)–O(2)–Pb(4)	104.5(5)			
P–Pb(1)	3.49(1)		Pb(4)–O(2)–Pb(4)	103.6(5)			
P–Pb(2)	3.92(1)						
P–Pb(2)	3.45(1)						
P–Pb(3)	3.54(1)						
P–Pb(4)	3.51(1)						

^aValence bond sums are indicated in bold.

constitute the equatorial plane of an octahedron with Pb(1) slightly out of that plane. The apexes are occupied by O(2) and one O(7) and they are tilted in the same direction away from the normal to the equatorial plane (Fig. 1b). The triangular face formed by O(7), O(5), O(8) is capped by a second O(7). The triangular face formed by the apex O(7) and atoms O(3), O(4) is open and the lone pair electrons cap this face. Pb(2), Pb(3), and Pb(4) have similar coordination polyhedra. The articulations of these distorted polyhedra lower the crystal symmetry to triclinic, $P\bar{1}$, as compared to the monoclinic structure of Pb₅SO₈ (14).

It is helpful to visualize this complex structure by describing it in terms of Pb polyhedra around oxygen atoms. Each O(1) and O(2) is tetrahedrally surrounded by four Pb (Table 4 and Fig. 2). Two O(1) that are centrosymmetrically related share a tetrahedral edge, Pb(3)–Pb(3), and two O(2) that are similarly related share a tetrahedral edge, Pb(4)–Pb(4). In turn the O(1) and O(2) tetrahedra share an edge, Pb(3)–Pb(4), to form chains along the *b*-axis (Fig. 2). The phosphate and Bi–O groups have tetrahedral and pentagonal pyramidal coordinations, respectively. O(6) and O(7) of PO₄ connect to Bi to form a chain parallel to the *b*-axis

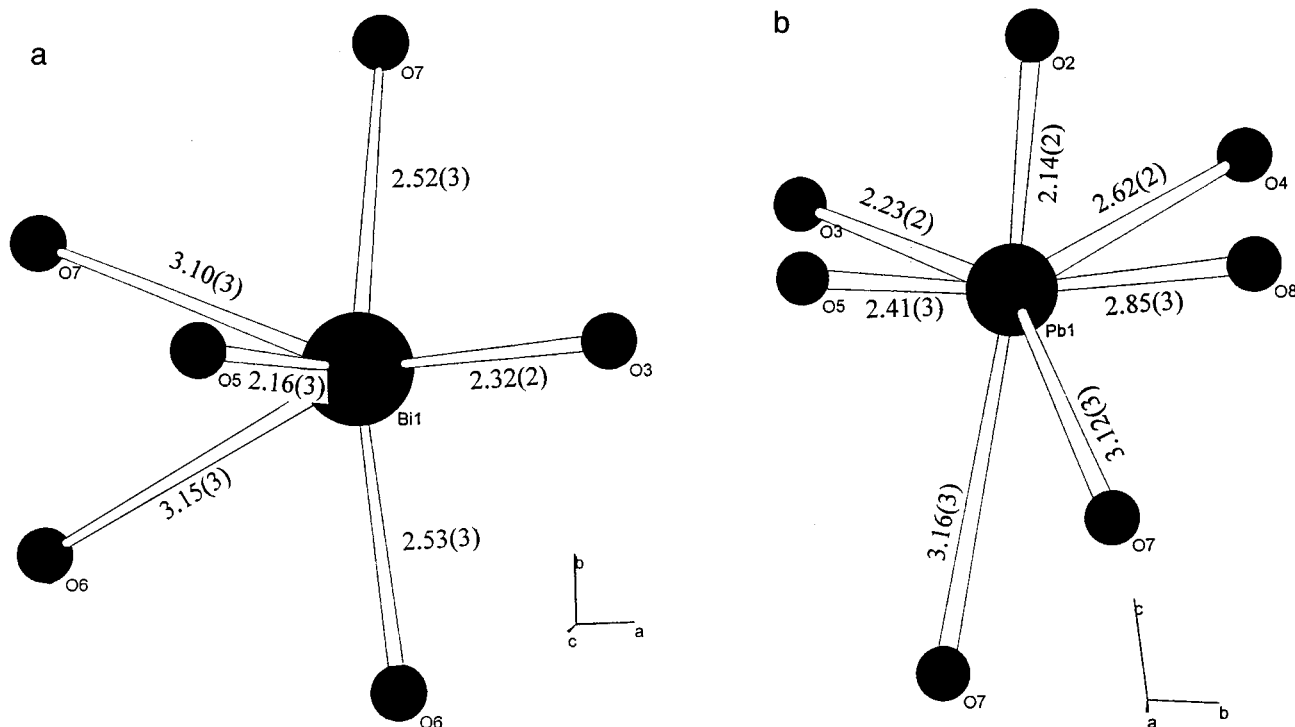


FIG. 1. (a). The oxygen atom environment around Bi seen along [001]. (b). The oxygen atom environment around Pb. Bond lengths and their standard deviations in Å.

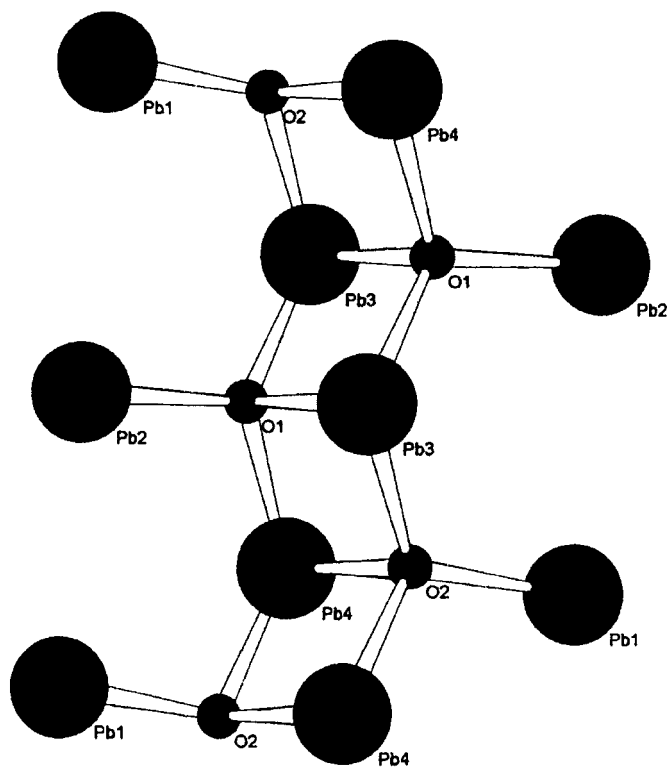


FIG. 2. The Pb environment around oxygen atoms O(1) and O(2).

(Fig. 3c). The apical O(8) of PO_4 and O(5) of the BiO_6 units are bonded to four Pb. In turn the Pb atoms also bond by van der Waals contacts to two O(7) or two O(6), giving rise to a two-dimensional plane parallel to (100) (Fig. 3). The Bi–Pb, Bi–P, and Pb–P bond lengths range from 3.45 to 3.92 Å, similar to those in related compounds (7, 14).

The Pb–O frameworks in tetragonal PbO (20), in Pb_5SO_8 (14), and in Pb_4BiPO_8 , (Figs. 3a–3c) display corrugated Pb–O chains. In PbO the chains are parallel to the *b*-axis and are linked so that the Pb atoms of two chains form a trigonal prism (Fig. 3a). In Pb_5SO_8 the chains are parallel to the *a*-axis and link to form a trigonal prism moiety that is distorted because the large SO_4 group alternates with Pb in the sixth position (Fig. 3b). In Pb_4BiPO_8 the sixth position is occupied by either Bi or PO_4 (Fig. 3c). In PbO the layers are linked by weak Pb–Pb van der Waals contacts. In Pb_5SO_8 (Fig. 4a), the parallel chains are linked by strong O–Pb–O bonds. Finally in Pb_4BiPO_8 (Fig. 4b), the basic units are linked by strong O(3)–Bi–O(5) bonds and weak O(6)–Bi (3.15 Å) and O(7)–Bi (3.10 Å) bonds. This Pb–O structural motif lends itself readily to the replacement of the PO_4 moiety by other tetrahedral groups such as SO_4 and AsO_4 and Bi by other trivalent ions of similar ionic radius. We, however, could not synthesize a hypothetical isostructural phase, Pb_4LaPO_8 .

Within experimental error the phosphorus atoms are in a nearly regular tetrahedral oxygen environment (Table 5),

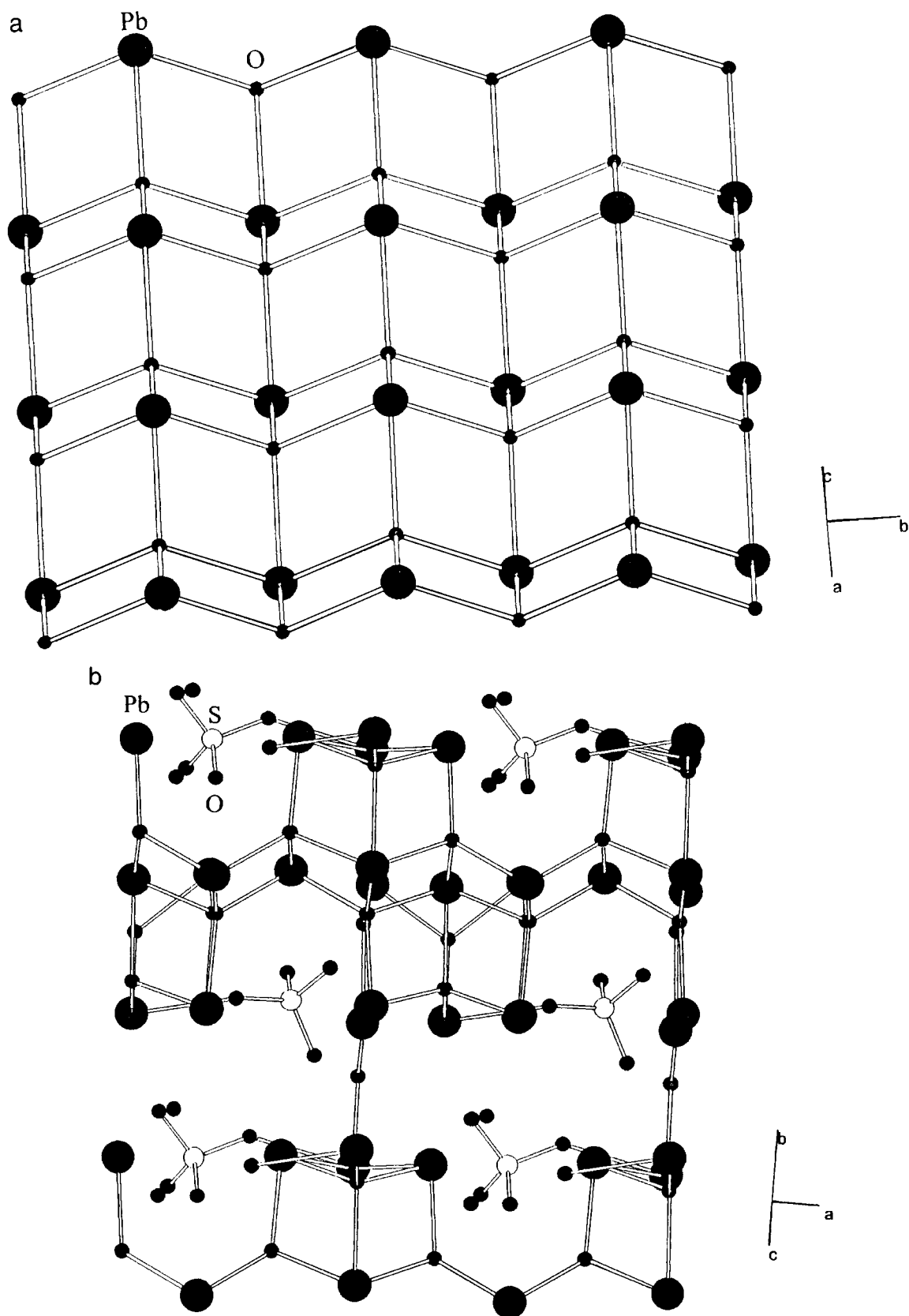


FIG. 3. The crystal structure motifs of (a) tetragonal PbO, (b) Pb_5SO_8 projected on (100), and (c) Pb_4BiPO_8 projected on (011).

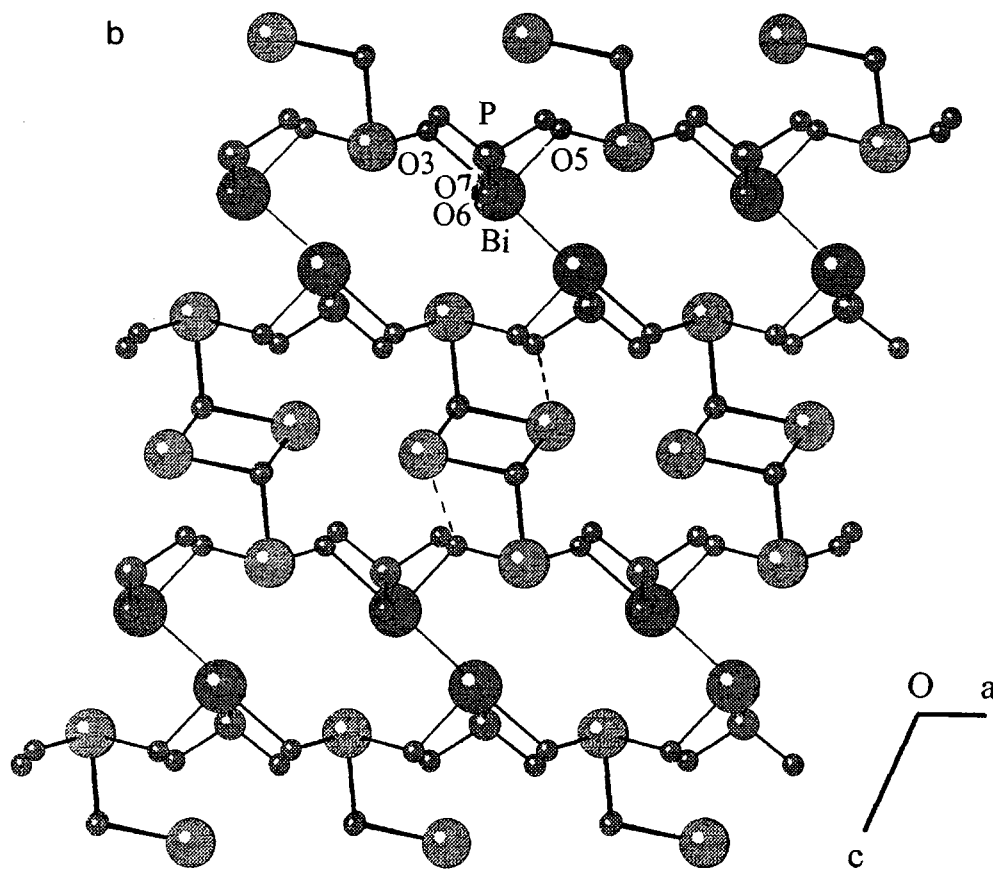


FIG. 4—Continued

with four P–O bond lengths contributing to a valence bond sum (21) of 5.14, close to the P^{5+} expected oxidation state. The Pb(1) oxygen coordination polyhedron has been previously described. The inclusion of these seven Pb–O bonds in the valence bond sum calculation yields 2.63, well over the 2^+ oxidation state. The valence bond sum calculated for Pb(2) is 2.32, while more normal values, 2.14 and 2.06, are calculated for Pb(3) and Pb(4). The valence bond sum for Bi is 2.14, much less than the expected trivalent oxidation state. Thus the high valence bond sums of Pb(1) and Pb(2) appear to compensate for the decrease of the Bi oxidation state. Interchanging Pb(1) and Bi leaves the structural parameters unchanged because of the nearly identical scattering power of the atoms. Further, such an interchange disrupts the Pb framework. We are certain that the atom assignment is correct. A low valence bond sum for Bi was observed in Pb_2BiPO_6 but there was compensated by an unusual 6.07 valence bond sum for P (7). Using the van der Waals radii for Pb and Bi as 2.02 and 1.82 Å, respectively, the contacts between Pb(1), Pb(2), and Bi are 3.73 Å but no contacts exist between Pb(3), Pb(4), and Bi. It is postulated that where van der Waals contacts for Pb–Bi exist the Pb $6s^2$ energy levels

overlap the empty Bi 6p energy levels so that electron transfer into the Bi 6p levels from Pb occurs. The electrons are not itinerant because of the large atomic separations and the material remains insulating.

ACKNOWLEDGMENTS

H.S. gratefully acknowledges the support of the R. A. Welch Foundation, Houston, Texas and S.G. thanks the IMCCEC/US consortium for a travel grant.

REFERENCES

1. V. V. Volkov, L. A. Zhreb, Y. F. Kargin, V. M. Skorikov, and I. V. Tananeav, *Russ J. Inorg. Chem.* **28**, 1002 (1983).
2. J. P. Wignacourt, M. Drache, P. Conflant, and J. C. Boivin, *J. Chim. Phys.* **88**, 1933 (1991).
3. Y. A. Blinovskov and A. A. Fotiev, *Russ. J. Inorg. Chem.* **32**, 145 (1987).
4. Akiteru Watanabe, *Solid State Ion.* **96**, 75 (1997).
5. A. Mizrahi, J. P. Wignacourt, M. Drache, and P. Conflant, *J. Mater. Chem.* **5**(6), 901 (1995).
6. Y. C. Jie and W. Eysel, *Powder Diffr.* **9**, 1 (1994).
7. A. Mizrahi, J. P. Wignacourt, and H. Steinfink, *J. Solid State Chem.* **133**, 516 (1997).

8. K. Sahl, *Z. Kristallogr.* **141**, 145 (1975).
9. B. F. Mentzen, J. C. Viala, A. Sartre, and J. Bouix, *C. R. Acad. Sci. Paris* **293**, Série II, 1053 (1981).
10. T. Negas, *J. Am. Ceram. Soc.* **51**, 716 (1968).
11. H. Bode and E. Voss, *Electrochim. Acta* **1**, 318 (1959).
12. Y. Watanabe and Y. Otsubo, *Nipp. Kagakukaishi* **8**, 1603 (1973).
13. D. B. Nihitjanova and V. I. Ivanov, *Z. Kristallogr.* **212**, 191 (1997).
14. Ian M. Steele and Joseph J. Pluth, *J. Electrochem. Soc.* **145**, 528 (1998).
15. P. E. Werner, L. Eriksson, and M. Westdahl, *J. Appl. Crystallogr.* **18**, 367 (1985).
16. G. M. Sheldrick, "SHELXTL Plus Crystallographic System." Siemens Analytical X-Ray Instruments, Madison, WI, 1989.
17. Sheldrick, "SHELXS86." Institut Anorganische Chemie, Göttingen, 1985.
18. G. M. Sheldrick, "SHELXL-93." Institut Anorganische Chemie, Göttingen, 1993.
19. Ron Jenkins and Robert L. Snyder, "Introduction to X-Ray Powder Diffractometry." Wiley, New York, 1996.
20. R. G. Wyckoff, "Crystal Structures," Wiley-Interscience, New York, 1963.
21. D. Brown and D. Altermatt, *Acta Crystallogr. B* **41**, 244 (1985).